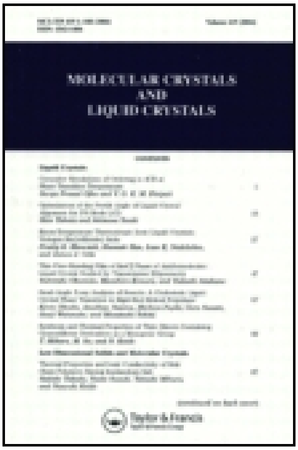

Molecular Crystals and Liquid Crystals
Publication details, including instructions for authors and subscription information:
http://www.tandfonline.com/loi/gmcl20

Liquid Crystalline Formation of Semifluorinated n-Alkanes FnHm; Molecular Dynamics Simulation Study Using Atomistic Model

Masakazu Fujiwara [a], Katsuhiko Satoh [b] & Shigeru Mita [c]

[a] KYOCERA Chemical Corporation, Ryoke, Kawaguchi, Saitama, Japan
[b] College of General Education, Osaka Sangyo University, Nakagaito, Daito, Osaka, Japan
[c] Department of Chemistry, Tokyo University of Science, Kagurazaka, Shinjuku, Tokyo, Japan

Version of record first published: 17 Oct 2011

To cite this article: Masakazu Fujiwara, Katsuhiko Satoh & Shigeru Mita (2005): Liquid Crystalline Formation of Semifluorinated n-Alkanes FnHm; Molecular Dynamics Simulation Study Using Atomistic Model, Molecular Crystals and Liquid Crystals, 441:1, 307-317

To link to this article: http://dx.doi.org/10.1080/154214091009987

Mol. Cryst. Liq. Cryst., Vol. 441, pp. 307–317, 2005
Copyright © Taylor & Francis Inc.
ISSN: 1542-1406 print/1563-5287 online
DOI: 10.1080/154214091009987

Liquid Crystalline Formation of Semifluorinated *n*-Alkanes FnHm; Molecular Dynamics Simulation Study Using Atomistic Model

Masakazu Fujiwara
KYOCERA Chemical Corporation, Ryoke, Kawaguchi, Saitama, Japan

Katsuhiko Satoh
College of General Education, Osaka Sangyo University,
Nakagaito, Daito, Osaka, Japan

Shigeru Mita
Department of Chemistry, Tokyo University of Science,
Kagurazaka, Shinjuku, Tokyo, Japan

A preliminary result for liquid crystalline formation of semifluorinated n-alkanes by a constant pressure molecular dynamics simulation using atomistic potential model has been reported. The system containing 256 molecules for semifluorinated n-alkanes was used. The change in the structure which was formed from an isotropic structure by cooling was investigated in this study. The systems studied formed layered structures spontaneously. Some of data on structure and density were found to be in concordance with that in experiments.

Keywords: atomistic model; molecular dynamics simulation; semifluorinated *n*-alkanes; smectic B phase

INTRODUCTION

Fluorocarbon and hydrocarbon are practically immiscible and are very different in a structural point of view. Fluorocarbons adopt a 15/7 helical structure by an intermolecular steric repulsion of the fluorine atoms along the carbon backbone, whereas hydrocarbons favor the well-known planar zigzag conformation. Semifluorinated *n*-alkanes

---

Address correspondence to Katsuhiko Satoh, College of General Education, Osaka Sangyo University, 3-1-1 Nakagaito, Daito, Osaka, 574-8530, Japan. E-mail: ksatoh@las.osaka-sandai.ac.jp

$F(CF_2)_n(CH_2)_mH$ (F*n*H*m*) which consist of their parts, consequently undergo mesophase-mesophase, mesophase-solid and/or solid-solid transitions [1–10]. Moreover, despite the missing of a hydrophilic head group, semifluorocarbons can form Langmuir films at the air–water interface, [11,12] is watched by diverse fields with keen interest [13,14]. These diblock molecules are of considerable interest because they have a different and unique structure from a normal mesogen containing a rigid core and flexible chains.

Reports on the structural characterization of semifluorinated *n*-alkanes have demonstrated that phase transition occurs with the molecules in lamellar structures [1–10,15,16]. In spite of the ample of experiments, the detailed packing model of the individual molecules within the lamellar is still unknown. Because it seems very difficult to observe the structural formation process of alkyl chains at the molecular level, such as the crystal growth process, by the present experimental techniques. Thus computer simulation is one of the strongest tools for investigating the mechanisms of the molecular packing in mesophase. In addition, an explicit treatment of molecular flexibility and electrostatic interactions by simulations in atomic model enables a detailed investigation of local molecular ordering in mesophase and comparison with experimental results. Several years ago, molecular dynamics simulations in atomistic level for Langmuir film of a semifluorinated *n*-alkane, F12H18 were carried by Kim and Shin, and spontaneous ordered structure formation were observed [17]. In addition, recently, we presented density behavior of F10Hm with m being an even number of carbon atoms ranging from 6 to 12 [18]. In this work, liquid crystalline formation of semifluorinated *n*-alkanes by a constant pressure molecular dynamics simulation using atomistic potential model has been reported.

COMPUTATIONAL DETAILS

The molecular dynamics simulations have been carried out with MDyna*mix* version 4.3 [19] with CHARMM force field type for the parallel computer IBM pSeries 690 of the computational center of Tokyo University of Science. The model semifluorinated *n*-alkane consists of CF_3, CF_2, CH_2, CH_3 groups, which are treated as united atoms. The total potential energy E_{total} is determined by the so-called force field as the sum of bonded atoms contributions including bending, E_{bend}, and Rychaert–Bellemans type torsional term, E_{torsion}, and of non-bonded Coulomb and Lennard-Jones, E_{nonbond}, term given by Eq. (1)–(3)

$$E_{\text{bend}} = \sum_{i=3}^{n} \frac{1}{2} k_\theta (\theta_i - \theta_0)^2 \tag{1}$$

$$E_{\text{torsion}} = \sum_{i=0}^{5} C_i \cos^i(\phi) + a\exp(-b\phi^2) \tag{2}$$

$$E_{\text{nonbond}} = \sum_{i}\sum_{j>i}\left\{\frac{q_i q_j e^2}{r_{ij}} + 4\varepsilon_{ij}\left[\left(\frac{\sigma_{ij}}{r_{ij}}\right)^{12} - \left(\frac{\sigma_{ij}}{r_{ij}}\right)^{6}\right]\right\} \tag{3}$$

where k_θ, a and b are force constants representing bond bending and torsional potentials respectively, and C_i is the rotational barrier. r_{ij} is a distance between interacting sites i and j. σ_{ij} is the parameter of the Lennard-Jones potential and q_i is the partial charge on site i. In this simulation, torsional motion for fluorocarbon chain is important because it forms 15/7 helical structure. In order to reproduce the structure in fluorocarbon chain, we used modified Rychaert–Bellemans potential by adding a corrective term, as Eq. (2) [17,20]. The values of all the potential parameters in the simulation are listed in Tables 1–3 [17,20,21]. The SHAKE algorithm was used for fixing bond lengths and to eliminate the high frequency bond stretching motion, so that it was possible to integrate the equations of motion with a time step of 5.0 fs. The simulated systems contained 256 molecules using rectangular cell by employing three dimensional periodic boundary conditions. The interactions were calculated with the minimum image convention using a cut-off radius of 1.3 nm. The simulations were performed in the isothermal-isobaric (*NPT*) ensemble by controlling Nosé-Hoover thermostat [22–24] and Parrinello-Rahman barostat [25]. Pressure was set equal to atmospheric pressure (1.0 atm) as same to experimental condition. Coulomb interactions were treated with EWALD summation method. Atomic charges for the electrostatic interactions were evaluated from theoretical calculation of *ab initio* MO method with B3LYP/6-311G** [26]. One of the optimized structures and the values for charge and dipole moment are shown in Figure 1 and Table 4. In order to examine dependence of the hydrocarbon chain

TABLE 1 Potential Energy Parameters

Parameter	Value	Unit
d_0	0.153	Nm
θ_0	110	degree
k_θ	460	kJ/rad^2 mol
a	14.0000	kJ/mol
b	12.7176	kJ/mol

TABLE 2 Values of the Coefficients in the Expansion of the Ryckaert-Bellemans Dihedral Potential

Atom	C_0	C_1	C_2	C_3	C_4	C_5
CF_2 and CF_3	15.1667	11.9444	–17.3333	4.4444	34.6667	–48.889
CH_2 and CH_3	9.2789	12.1557	–13.1201	–3.0597	26.2403	–31.4950
CF_2 and CH_2	11.7644	12.6800	–15.2356	–0.6400	30.4711	–39.0400
CF_2(helix)	14.8240	11.2778	–12.0000	9.7778	24.0000	–59.5556

(Unit in $kJ\,mol^{-1}$)

TABLE 3 Values of the Lennard-Jones Parameters

Atom	ε/K	σ/nm
$CH_2–CH_2$	70.4	0.3965
$CH_3–CH_3$	90.7	0.3786
$CF_3–CF_2$	40.5	0.5078
$CF_3–CF_3$	57.6	0.5078

length, a number of carbon for fluorocarbon was fixed to n of 10 and a number of carbons for alkyl chains m of 6, 8, 10 and 12 were used in this study. Relatively long run of 5.0 ns was carried out for each system to monitor a liquid crystalline formation from isotropic structure. Initially, perfect aligned configurations were used to melt for a starting configuration. The system was heated up to be an isotropic structure gradually as shown in Figure 2, and then the obtained isotropic structures were used as a starting configuration of the simulations.

RESULTS AND DISCUSSION

Figure 3 shows that the change in the configurational snapshots after cooling at 330 K from 400 K for F10H6. As can been seen, the structure drastically changed at this temperature as time went by. A layered

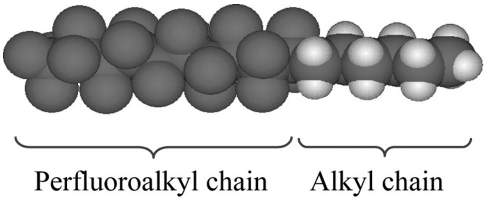

FIGURE 1 The optimized structure for F10H6 by *ab initio* MO calculation with B3LYP/6-311G**.

TABLE 4 Optimized Values of Atomic Charges and Dipole Moment for F10H6

Atom	Charge
CF_3	0.119
CF_2	–0.097
CF_2	–0.021
CF_2	–0.005
CF_2	–0.004
CF_2	–0.003
CF_2	–0.010
CF_2	0.005
CF_2	–0.035
CF_2	–0.067
CH_2	0.060
CH_2	0.034
CH_2	0.006
CH_2	0.005
CH_2	–0.013
CH_3	0.025
Dipole	2.97 Debye

structure was spontaneously formed from an isotropic structure in a few ns. Although there are some molecules between layers, most molecules aligned uniformly. For other systems with different length of alkyl chain, similar layered structures were also formed at different temperatures. As describe below, the transition temperature was decreased as alkyl chain length was shorten as experiments. This means that it is possible to discuss a dependence of alkyl chain length on the transition of liquid crystal phase from isotropic phase by the simulation using the atomistic model. According to the experiments, these compounds take a smectic B phase from isotropic phase directly [3–5,16,18]. No nematic phase forms for a series of the compounds. Therefore, the transition behavior in the simulation was the same as that in experiments. The snapshots say that most molecules change all-trans conformation first, and then the elongated molecules move to arrange for the ordered structure. The change in potential energy during the ordering process is shown for F10H6 in Figure 4. At initial stage, the potential energy fluctuated, and then the energy decreased quickly until at about 1.5 ns. This rate depends on the cooling speed. In this case, the layer structure starts to form gradually at t of 0.75 ns by the snapshots, and then the final layered structure formed after 1.5 ns. After 1.5 ns, the energy reaches equilibrium state with thermal fluctuation. In experiment, dependence of the chain length on the kinetic behavior at the transition was observed [18]. However, the

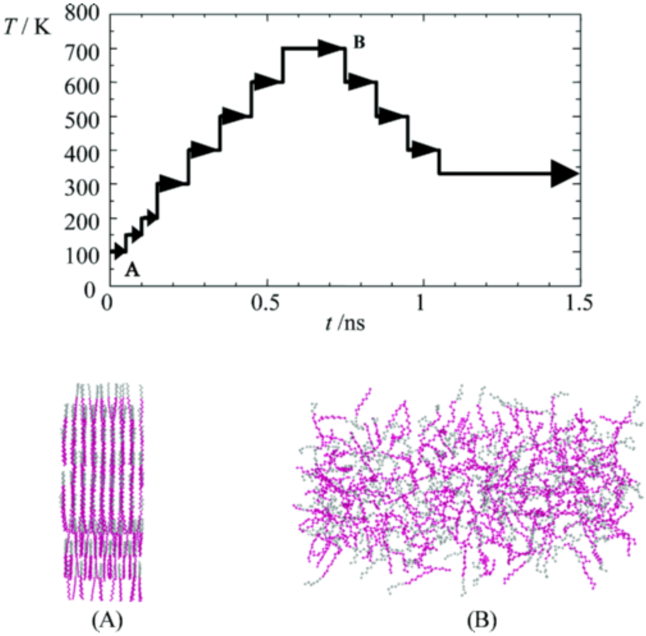

(A) (B)

FIGURE 2 Scheme for temperature change in the simulation for preparing a starting configuration for F10H6. Dark colored part indicates fluorinated chain, and bright colored part indicates hydrocarbon segment in the snapshots. The perfect aligned configuration A was melted by heating process from 100 K to 700 K, and then the obtained random structure B was used for the simulation as a starting configuration.

transition rate is not so easy to determine because of the rapid cooling speed in the simulation. For the system for F10H12, unique structure was formed at 320 K. Figure 5 shows a snapshot of equilibrium state for the system. In case of F10H12, specific structure of mixture for monolayer and bilayer structures was obtained in an equilibrium structure. In fact, two peaks have also been observed for F10H12 and F10H13 in a small-angle X-ray experiment [18]. These two peaks suggest that two kinds of layer structures exist. The mixed structure obtained from the simulation seems to be identified to the structure measured in experiment. Moreover, the kind of structure was not formed in the simulations for other systems of F10H6, F10H8 and F10H10, which was in concordance with the experimental data [18]. In the bilayer region, the hydrocarbon segments are interdigitated although there are some irregular molecules, and the fluorinated carbon segments aggregate between layers in the simulation. At least,

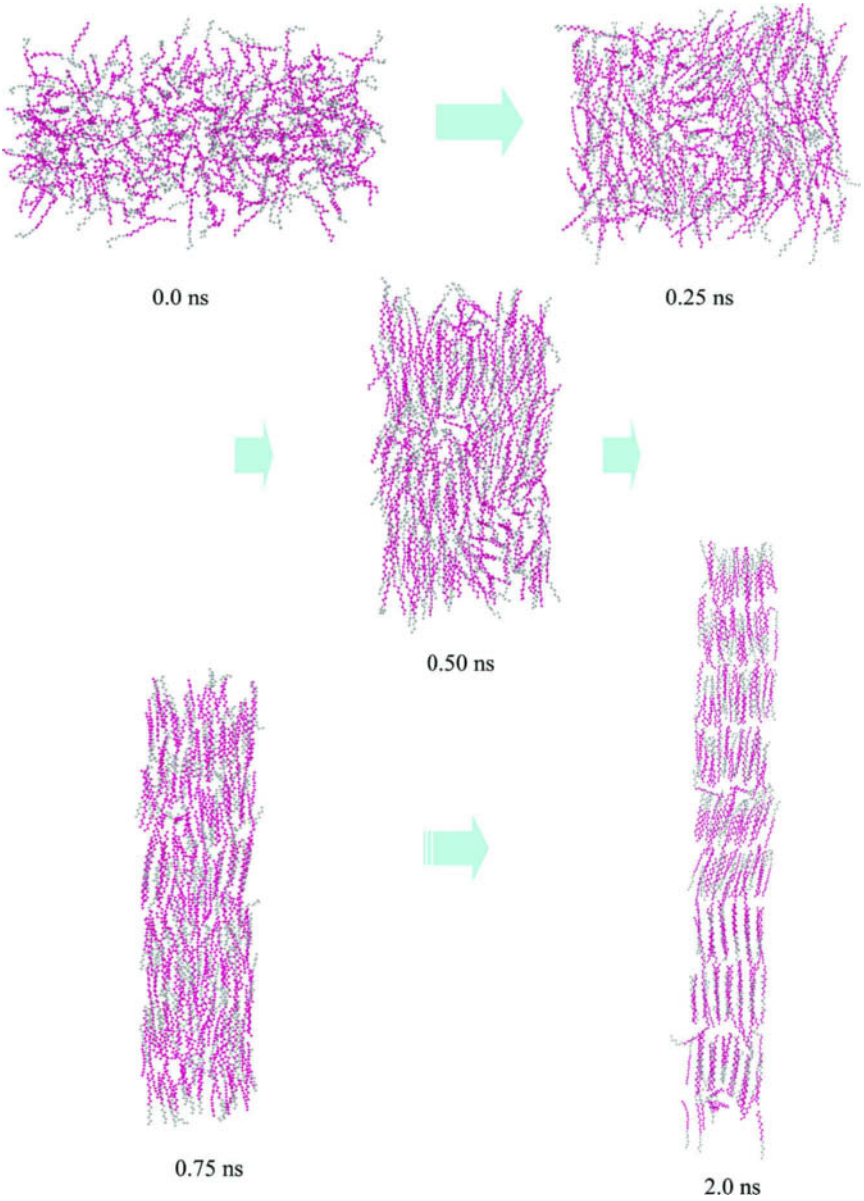

FIGURE 3 The configurational snapshots during the ordering process at 330 K for F10H6. Dark colored part indicates fluorinated chain, and bright colored part indicates hydrocarbon segment.

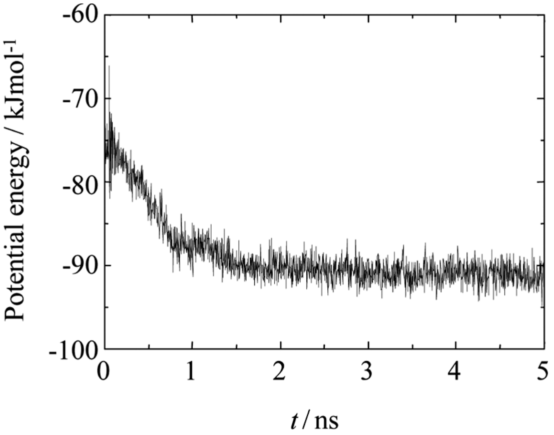

FIGURE 4 Time evolution of potential energy during the ordering process at 330 K for F10H6.

same segments seem to aggregate in the bilayer structure. On the other hand, there is no significant specific rule for the arrangement in the monolayer region. Formation of the mixed structure seems to be caused by kinetic reason and relationship of chain length between fluorinated and hydrocarbon segments. In order to examine this, simulation of formation from isotropic structure is desired because the system for the flexible long chain molecules has a complicated potential energy surface. It was difficult to monitor the behavior in the melting process from the system in which the molecules aligned. At this point, the potential parameter set and the simulation for the flexible atomistic model are important.

In experiment, the change in the density for the compounds has been measured precisely by dilatometry [18]. The range of the density for the compounds are 1.35–1.7 g cm^{-3} [18]. The change in the density for the system are shown in Figure 6. The changes in the simulation are much simpler than that in experiment due to rapid temperature changing. However, the values of the density in the isotropic phase and the ordered phase which has layer structure were comparable to the real values, and then dependence of chain length for alkyl segment was also in agreement with that in experiment. Therefore, the system studied can be possible to examine the packing condition for the system by considering cooling rate. Actually the obtained structures from isotropic phase depended on the cooling rate and the initial configurations presumably. Therefore, careful choice of cooling rate and starting configuration are required in the simulations. In addition,

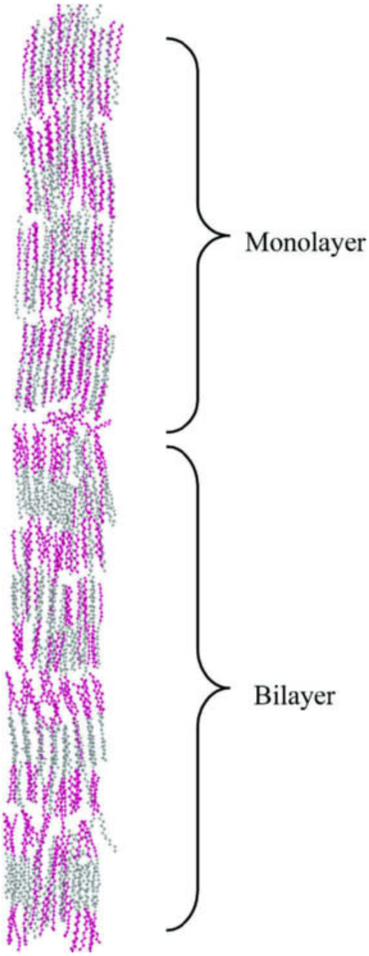

FIGURE 5 The configurational snapshot at 320 K for F10H12. Dark colored part indicates fluorinated chain, and bright colored part indicates hydrocarbon segment.

detail analysis for structure and dynamics are desired. The detail analysis is under way.

SUMMARY

A constant pressure molecular dynamics simulation using atomistic model has been performed for semifluorinated n-alkanes. The united atoms were used for CH_2, CH_3, CF_2 and CF_3 parts for computational

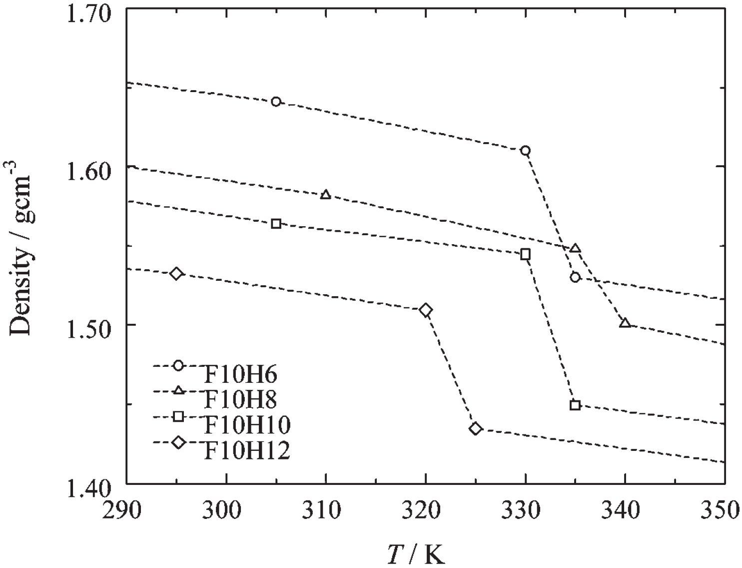

FIGURE 6 The temperature dependence of the density for the systems studied. The circle, triangle, square and diamond symbols are values of density in the simulation for F10H6, F10H8, F10H10 and F10H12, respectively.

efficiency. The values for atomic charges were evaluated by *ab initio* MO method with B3LYP/6-311G**. The length for perfluorinated carbon was fixed and the length for hydrocarbon chain was changed from 6 to 12. All systems studied were found to form highly ordered structures with layers by cooling from a random structure at high temperature. The phase structure depended on the length of a hydrocarbon. The mixture of monolayer and bilayer structures which was observed in X-ray experiment were reproduced in the simulation for F10H12. In addition, another molecules formed only monolayer structure as the same as the results in the experiment.

The values were not only comparable with the real experimental values, but the dependence of alkyl chain length on the change in the density was also in agreement with that in experiment quantitatively, although it is not possible to discuss at low temperature region because the cooling manner in the simulation was not so fine. The potential parameter set and the system in the study are useful to investigate behavior of molecular arrangement and aggregation of flexible molecules. Further, discussion of dependence of alkyl chain length on the transition behavior and packing process from isotropic phase could be possible by considering cooling rate. Therefore, the detail analysis for structure and dynamics for the systems would be required in future works.

REFERENCES

[1] Rabolt, J. F., Russell, T. P., & Twieg, R. J. (1984). *Macromolecules*, *17*, 2786.

[2] Russell, T. P., Rabolt, J. F., Twieg, R. J., Siemens, R. L., & Farmer, B. L. (1986). *Macromolecules*, *19*, 1135.

[3] Mahler, W., Guillon, D., & Skoulios, A. (1985). *Mol. Cryst. Liq. Cryst. Lett.*, *2*, 111.

[4] Viney, C., Russell, T. P., Depero, L. E., & Twieg, R. J. (1989). *Mol. Cryst. Liq. Cryst.*, *63*, 168.

[5] Viney, C., Twieg, R. J., Russell, T. P., & Depero, L. E. (1989). *Liq. Cryst.*, *5*, 1783.

[6] Höpken, J., Pugh, C., Richtering, W., & Möller, M. (1988). *Makromol. Chem.*, *189*, 911.

[7] Höpken, J. & Möller, M. (1992). *Macromolecules*, *25*, 2482.

[8] Marczuk, P. & Lang, P. (1998). *Macromolecules*, *31*, 9013.

[9] Marczuk, P., Lang, P., & Möller, M. (2000). *Colloid and Surfaces A*, *163*, 103.

[10] Geppi, M., Pizzanelli, S., Veracini, C. A., Cardelli, C., Tombari, E., & Nostro, P. L. (2002). *J. Phys. Chem. B*, *106*, 1598.

[11] Gaines, G. L., Jr. (1991). *Langmuir*, *7*, 3054.

[12] El Abed, A., Pouzet, E., Fauré, M-C., Sanière, M., & Abillon, O. (2000). *Phys. Rev. E*, *62*, 5895.

[13] Tamada, K., Ishida, T., Knoll, W., Fukushima, H., Colorado, R., Jr., Graupe, M., Shmakova, O. E., & Lee, T. R. (2001). *Langmuir*, *17*, 1913.

[14] Wong, D. & Lois, N. (2000). *Semin Ophthalmol*, *15*, 25.

[15] Araki, K., Satoh, K., & Kondo, S. (1996). *Mol. Cryst. Liq. Cryst.*, *281*, 123.

[16] Araki, K., Satoh, K., & Kondo, S. (1997). *Mol. Cryst. Liq. Cryst.*, *302*, 369.

[17] Kim, N. & Shin, S. (1999). *J. Chem. Phys.*, *111*, 6556.

[18] Fujiwara, M., Satoh. K., Kondo, S., & Ujiie. S., submitted for publication.

[19] Lyubartsev, A. P. & Laaksonen, A. (2000). *Comput. Phys. Commun.*, *128*, 565.

[20] Shin, S. & Rice, S. A. (1994). *Langmuir*, *10*, 262.

[21] Ryckaert, J. P. & Bellemans, A. (1978). *J. Chem. Soc., Faraday Discuss.*, *66*, 95.

[22] Nosé, S. (1984). *J. Chem. Phys.*, *81*, 511.

[23] Nosé, S. (1984). *Mol. Phys.*, *52*, 255.

[24] Hoover, W. G. (1985). *Phys. Rev. A*, *31*, 1695.

[25] Parrinello, M. & Rahman, A. (1981). *J. App. Phys.*, *52*, 7182.

[26] Gaussian 03, Revision B.03, Frisch, J., Trucks, G. W., Schlegel, H. B., Scuseria, G. E., Robb, M. A., Cheeseman, J. R., Montgomery, J. A., Jr., Vreven, T., Kudin, K. N., Burant, J. C., Millam, J. M., Iyengar, S. S., Tomasi, J., Barone, V., Mennucci, B., Cossi, M., Scalmani, G., Rega, N., Petersson, G. A., Nakatsuji, H., Hada, M., Ehara, M., Toyota, K., Fukuda, R., Hasegawa, J., Ishida, M., Nakajima, T., Honda, Y., Kitao, O., Nakai, H., Klene, M., Li, X., Knox, J. E., Hratchian, H. P., Cross, J. B., Adamo, C., Jaramillo, J., Gomperts, R., Stratmann, R. E., Yazyev, O., Austin, A. J., Cammi, R., Pomelli, C., Ochterski, J. W., Ayala, P. Y., Morokuma, K., Voth, G. A., Salvador, P., Dannenberg, J. J., Zakrzewski, V. G., Dapprich, S., Daniels, A. D., Strain, M. C., Farkas, O., Malick, D. K., Rabuck, A. D., Raghavachari, K., Foresman, J. B., Ortiz, J. V., Cui, Q., Baboul, A. G., Clifford, S., Cioslowski, J., Stefanov, B. B., Liu, G., Liashenko, A., Piskorz, P., Komaromi, I., Martin, R. L., Fox, D. J., Keith, T., Al-Laham, M. A., Peng, C. Y., Nanayakkara, A., Challacombe, M., Gill, P. M. W., Johnson, B., Chen, W., Wong, M. W., Gonzalez, C., & Pople, J. A. (2003). *Gaussian, Inc.*, Pittsburgh: PA.